

# Imposing joint kinematic constraints with an upper limb exoskeleton without constraining the end-point motion

V. Crocher, A. Sahbani and G. Morel

**Abstract**— One of the key features of upper limb exoskeletons is their ability to take advantage of the human arm kinematic redundancy in order to modify the subject's joint dynamics without affecting his/her hand motion. This is of particular interest in the field of neurorehabilitation, when an exoskeleton is used to interact with a patient who suffers from joint motions desynchronization, resulting *e.g.* from brain damage following a stroke.

In this paper, we investigate this problem from the robot control point of view. A first general controller is derived which uses viscous force fields in order to generate joint torques counteracting any velocities that are perpendicular to a given set of constraints. In order to minimize energy dissipation, a second controller is proposed that still uses viscous force fields, but in a way that the mechanical power dissipated by the viscous control is null at any time. This controller does not impose any trajectory to the hand and the robot only moves in response to the forces generated by the patient.

This approach is experimented on a 4-DOF exoskeleton with a healthy subject. Results exhibit the basic properties of the controller and show its capacity to impose an arbitrary chosen joint constrain for 3-DOF pointing tasks without constraining the hand motion.

## I. INTRODUCTION

Neuro-rehabilitation is one of the developing applications for interactive robotic devices. Indeed, following a stroke, which is widely stated as the most common cause of complex disability, brain damages may appear and induce motor troubles. In this case, pharmacology is of very little help. Rather, physical therapy involving repetitive motor exercises is largely recognized as the only possible option. Therapy efficiency depends on its intensity and reactivity after the accident [1], [2]. This is why robotic assistance, providing the ability of finely controlling forces and movements in a repetitive manner, has been considered in the past years as a possible way to help a patient better recovering motor control capabilities. Usefulness of robotic systems in rehabilitation has been shown by several studies [3] [4]. Pioneer devices, such as the MIT Manus [5], have already been used for clinical therapies. Their benefit, in complement of classical rehabilitation, has been proven. These pioneer works have identified a crucial feature that the robotic device shall offer: the ability of fine interaction with the patient. In particular the motivation, interest and intention in patient's movements are fundamental for the recovery [6]. Among possible robotic devices, exoskeleton structures are of particular interest,

since they offer the opportunity to interact at the joint level with a patient [7]. This shall provide means to help patients recovering not only end point (hand) motion control, but also acceptable *joint synchronization*. It is indeed often observed on many post stroke patients that the kinematic redundancy of the arm is not solved properly by the central nervous system, leading in pathologic postures of the limb during motions [8], [9]. Correcting the so-called *synergies* between arm joints is so essential. A synergy is a coordination during movement and could be expressed in several spaces : muscular activity, joint velocities or joint torques. Bernstein [10] explained the existence of synergies as a solution for motor control system to resolve redundancy: *the co-ordination of a movement is the process of mastering redundant degrees of freedom of the moving organ, in other words its conversion to a controllable system.*

In the literature, research in developing upper-limb robotic rehabilitation exoskeletons, with the capacity of 3D interaction at joint level, primarily focuses on design. Different technologies are used. SUEFUL 7, a 7-DOF exoskeleton [11] and the 4-DOF Delaware exoskeleton [12] are actuated by cables, whereas some others like Rupert [13],[14] or the 7-DOF "Soft-actuated" exoskeleton [15] used pneumatic muscles. ARMin [16], [17] and ABLE [18], the 4-DOF exoskeleton used for the experiments in this paper, are activated electrically.

Regarding the control aspects, literature provides solutions that adapt end-point controllers to the joint space problem. For example, impedance control was originally used for rehabilitation on a planar manipulandum, which guides the patient's hand around a predefined trajectory in [19]; it was lately applied to assisting the shoulder joint motions thanks to an exoskeleton in [20]. Another type of joint space impedance control (force fields) is proposed within the ARMin project in [17], where the nominal trajectory is calculated from the minimum jerk criterion [21]. This last research is motivated by the need of defining ecologic movements at both the end-effector level and the end-point level.

For all these previous controllers, a drawback lies in the necessity of defining a desired trajectory prior to the movement, which is somehow contrary to the need of respecting intended movement from the patient. Indeed, it seems preferable to implement a controller where the final goal of the movement is not known in advance. Furthermore, these different exoskeleton control modes do not explicitly take into account the arm joint coordination problem.

The authors are with Institute of Intelligent Systems and Robotics (CNRS - UMR 7222), University Pierre & Marie Curie, Paris, France [crocher,sahbani,morel@isir.fr](mailto:crocher,sahbani,morel@isir.fr)

To overcome these difficulties, an original controller is proposed in the present paper, aiming at correcting joint coordination without constraining hand motion. Firstly, the force fields used are exclusively viscous (joint forces depend only on joint velocities). Therefore, there is no need for any pre-computed reference trajectory and the controller is purely reactive to patient's intended motions. Note that in order to ease motions when the patient motor capabilities are still limited, the programmed viscous force field is optionally non dissipative. Secondly, the force field itself is computed from the explicit formulation of joint space kinematic constraints, which, to our knowledge, is not featured by any other exoskeleton controllers proposed so far.

Section II details the proposed approach and the control algorithms while Section III describes the first experimental results obtained on a given exoskeleton, called ABLE [18].

## II. PROPOSED APPROACH

### A. Kinematic constraints

Models used in the literature for the human arm kinematics include from 7 to more than 10 joint DOFs depending whether or not they include the mobility of the scapula. Therefore, whatever the hand task, there is always an infinite number of solutions for the arm joint movements. In this paper, we are focused on the control of an exoskeleton, *i.e.* a robotic system attached to the arm, which kinematics approximates those of the human arm. We will note  $n$  the number of active joints of the exoskeleton, and  $m$  the number of independent kinematic parameters involved by the task to be performed. For example, if the subject is asked to point a given location in space with a rod, without any constraint on the orientation,  $m$  will be equal to 3.

When  $n > m$ , the task is redundant also from the exoskeleton point of view. Assume that the exoskeleton is in a completely transparent mode, that is it has the capability of not resisting to any intended motion of the subject. When the subject performs a task, the exoskeleton motion is then equal to the motion that the subject would perform under free condition. In particular, the joint synchronization algorithm used to solve the redundancy is produced by the subject's Central Nervous System. We consider in the next that we want the robot to affect these natural synergies. It is assumed that this can be express by imposing  $l \leq n - m$  scalar constraints to the robot joint velocity vector  $\dot{\mathbf{q}} \in \mathbb{R}^n$ .

More precisely, the different constraints are defined as a set of  $C^1$  scalar constraints  $f_i(\dot{\mathbf{q}}) = 0$  that can be grouped in a vector function  $\mathbf{F} : \mathbb{R}^n \rightarrow \mathbb{R}^l$ :

$$\mathbf{F}(\dot{\mathbf{q}}) = \begin{bmatrix} f_1(\dot{\mathbf{q}}) \\ \vdots \\ f_i(\dot{\mathbf{q}}) \\ \vdots \\ f_l(\dot{\mathbf{q}}) \end{bmatrix} = \mathbf{0} \quad , \quad (1)$$

where  $l \in \{1, \dots, n - m\}$  is the number of constraints.

### B. Torque control

The proposed control law is developed in joint space. It is assumed that the device is torque-controllable *i.e.* the control input to the system is vector  $\tau_m \in \mathbb{R}^n$  regrouping  $n$  joint motor torques  $\tau_{m_i}, i \in \{1, \dots, n\}$ . Note that position controlled devices, where the control input is a position vector, exhibit low backdrivability, and are not well suited for the type of applications targeted by this work.

In order to be able to apply on exoskeleton joints a torque command, it is essential to eliminate perturbations due to the robot dynamics. Indeed the robot arm has its own weight and actuators exhibit friction. At its lowest level, the control law is composed of three different terms:

- A gravity compensation torque  $\tau_g$ , calculated from joints positions and robot elements masses;
- A friction compensation torque  $\tau_f$ , calculated from joints speeds and actuators viscosity identification;
- A commanded torque  $\tau_c$ .

The motor torque  $\tau_m$  is the sum of these three torques :

$$\tau_m = \tau_g + \tau_f + \tau_c \quad , \quad (2)$$

as shown on Fig. 1.

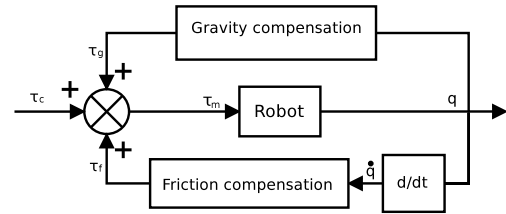


Fig. 1. The control loop with the three different torques.

### C. Elastic vs viscous fields

Mainly two kinds of force fields can be used for imposing kinematic constraints: elastic fields and viscous fields. In the case of elastic fields, the joint torque  $\tau$  is computed by:

$$\tau = -k(\mathbf{q}_0 - \mathbf{q}) \quad , \quad (3)$$

where  $\mathbf{q}_0$  is a reference joint position. Integrating the constraints given by Eq. (1) into this type of controller is classically done when computing  $\mathbf{q}_0$ : given an initial value  $\mathbf{q}_{init}$  for  $\mathbf{q}$  and a final value for the task function  $\mathbf{x} \in \mathbb{R}^m$ , one can first interpolate for  $\mathbf{x}$  and then solve for the inverse kinematics by explicitly integrating Eq. (1). This is suitable for conventional robot control, but it requires an a priori knowledge on the task trajectory  $\mathbf{x}(t)$ . We here want to implement a reactive controller without any a priori knowledge on the motion intended by the patient.

In this work, we proposed viscous force field based control law. Nevertheless, it is quite possible to combine viscous and elastic fields. In our case, the applied torque is defined by :

$$\tau = -\mathbf{K}\dot{\mathbf{q}} \quad (4)$$

where  $\mathbf{K} \in \mathbb{R}^{n \times n}$  is a viscosity matrix. Note that  $\mathbf{K}$  is not necessarily constant, nor diagonal. In the next section, we show how this control law is computed in order to impose constraints defined by Eq. (1).

#### D. Explicit integration of kinematic constraints into viscous fields

Assume that the exoskeleton is moved by the subject. At a given time, the joint velocity is  $\dot{\mathbf{q}}$ . If  $\mathbf{F}(\dot{\mathbf{q}}) = \mathbf{0}$ , then the resistive torque shall be null, because the subject's motion satisfies the constraints. In any other case, the velocity shall be corrected. Namely, we shall find the velocity correction  $\delta\dot{\mathbf{q}}$  such that:

$$\mathbf{F}(\dot{\mathbf{q}} + \delta\dot{\mathbf{q}}) = \mathbf{0} \quad (5)$$

Assuming small corrections, we obtain :

$$\mathbf{F}(\dot{\mathbf{q}} + \delta\dot{\mathbf{q}}) - \mathbf{F}(\dot{\mathbf{q}}) \approx \mathbf{J}\delta\dot{\mathbf{q}}, \quad (6)$$

where  $\mathbf{J}$  is the jacobian matrix of  $\mathbf{F}(\dot{\mathbf{q}})$ , defined as :

$$\mathbf{J}_{i,j} = \left( \frac{\partial f_i}{\partial \dot{q}_j} \right). \quad (7)$$

In order to satisfy Eq. (5), we have to compute  $\delta\dot{\mathbf{q}}$  such that:

$$-\mathbf{F}(\dot{\mathbf{q}}) = \mathbf{J}\delta\dot{\mathbf{q}}, \quad (8)$$

Among all the possible solutions, it seems interesting to compute the smallest one (having the smallest norm), because this will minimize the exoskeleton correction. This correction could be formulated as :

$$\delta\dot{\mathbf{q}} = -\mathbf{J}^+\mathbf{F}(\dot{\mathbf{q}}), \quad (9)$$

where  $\mathbf{J}^+$  is the pseudo-inverse of the jacobian matrix :

$$\mathbf{J}^+ = \mathbf{J}^T (\mathbf{J}\mathbf{J}^T)^{-1}. \quad (10)$$

Finally, applied torques on the controller are given by :

$$\tau_{c1} = k\delta\dot{\mathbf{q}} = -k\mathbf{J}^+\mathbf{F}(\dot{\mathbf{q}}) \quad (11)$$

where  $k$  is a scalar viscosity factor.

Obviously, this torque will be null when  $\mathbf{F}(\dot{\mathbf{q}}) = \mathbf{0}$ . In other cases, when a torque  $\tau_{c1} \neq \mathbf{0}$  is applied, we have in general  $\tau_{c1}^T \dot{\mathbf{q}} < 0$ , meaning that the exoskeleton dissipates energy. In order to avoid energy dissipation, an additional component to the control torque is introduced in the next paragraph.

#### E. Non dissipative viscous fields

The main idea is to add a torque that encourages motions satisfying the constraints. A second torque, noted  $\tau_{c2}$ , is introduced. The objective is to amplify the part of the velocity that satisfies the constraint, namely  $(\dot{\mathbf{q}} - \mathbf{J}^+\mathbf{F}(\dot{\mathbf{q}}))$ . The later could be seen as an orthogonal projection of the velocity on the orthogonal direction of the constraint.  $\tau_{c2}$  could be then expressed as follows :

$$\tau_{c2} = k\alpha (\dot{\mathbf{q}} - \mathbf{J}^+\mathbf{F}(\dot{\mathbf{q}})) \quad (12)$$

where  $\alpha$  is a scalar modulation. Clearly, large values of  $\alpha$  would lead to instability because a large positive feedback

will be induced. In our case,  $\alpha$  is computed in order to obtain no energy dissipation. For that :

$$(\tau_{c1} + \tau_{c2})^T \dot{\mathbf{q}} = 0 \quad (13)$$

Solving equation (13), we obtain :

$$\alpha = \begin{cases} 0 & \text{if } (\|\dot{\mathbf{q}}\|^2 - \dot{\mathbf{q}}^T \mathbf{J}^+ \mathbf{F}(\dot{\mathbf{q}}) = 0) \\ -\frac{\dot{\mathbf{q}}^T \mathbf{J}^+ \mathbf{F}(\dot{\mathbf{q}})}{\|\dot{\mathbf{q}}\|^2 - \dot{\mathbf{q}}^T \mathbf{J}^+ \mathbf{F}(\dot{\mathbf{q}})} & \text{otherwise} \end{cases} \quad (14)$$

In order to modulate the amount of encouraging torque  $\tau_{c2}$ , a coefficient  $\epsilon \in [0, 1]$  is set. The final controller is thus:

$$\tau_c = -k [\mathbf{J}^+ \mathbf{F}(\dot{\mathbf{q}}) - \epsilon\alpha (\dot{\mathbf{q}} - \mathbf{J}^+ \mathbf{F}(\dot{\mathbf{q}}))] \quad (15)$$

#### F. Linear case

In the particular case of linear constraints,  $\mathbf{F}(\dot{\mathbf{q}})$  could be expressed as:

$$\mathbf{C}\dot{\mathbf{q}} = 0 \quad (16)$$

with  $\mathbf{C} \in \mathbb{R}^{l \times m}$ . In this case, since  $\mathbf{J} = \mathbf{C}$ , equations (11) and (12) became :

$$\tau_{c1} = -k\mathbf{C}^+\mathbf{C}\dot{\mathbf{q}}; \quad (17)$$

$$\tau_{c2} = k\alpha (\mathbf{I} - \mathbf{C}^+\mathbf{C}) \dot{\mathbf{q}}, \quad (18)$$

where:

$$\alpha = \begin{cases} 0 & \text{if } (\dot{\mathbf{q}}^T \mathbf{C}^+ \mathbf{C} \dot{\mathbf{q}} - \|\dot{\mathbf{q}}\|^2 = 0) \\ \frac{\dot{\mathbf{q}}^T \mathbf{C}^+ \mathbf{C} \dot{\mathbf{q}}}{\dot{\mathbf{q}}^T \mathbf{C}^+ \mathbf{C} \dot{\mathbf{q}} - \|\dot{\mathbf{q}}\|^2} & \text{otherwise} \end{cases}; \quad (19)$$

and finally, the applied torque is the sum of  $\tau_{c1}$  and  $\tau_{c2}$  :

$$\tau_c = -k [\mathbf{C}^+ \mathbf{C} + \epsilon\alpha (\mathbf{I} - \mathbf{C}^+ \mathbf{C})] \dot{\mathbf{q}} \quad (20)$$

In order to illustrate the velocities projections and the calculated torques, Figure 2 presents a simple case where  $n = 2$ ,  $l = 1$  and  $m = 1$ . The constraint matrix chosen here is  $\mathbf{C} = [-1 \ 3]$  while  $\epsilon = 1$ .

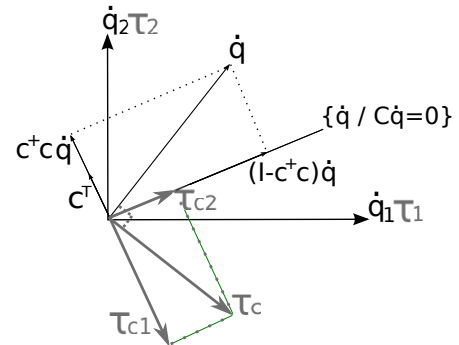


Fig. 2. Representation of the projections in the case of  $\mathbf{C} = [-1 \ 3]$ .

### III. EXPERIMENTAL VALIDATION

To validate this control mode, we will experimentally demonstrate the ability of the exoskeleton ABLE to impose a joint speed coordination to a healthy subject while keeping unchanged the main characteristics of the endpoint movements. If the control allows to change a natural coordination of a healthy subject, it can correct the joint coordination of a patient.

#### A. ABLE

ABLE is a 4-DOF exoskeleton developed by CEA-LIST [18]. All the four DOF are actuated by a motor and a screw-cable mechanical transmission. Optical incremental encoders mounted on each joint enable the calculation of joint positions and joint speeds by derivation. The three first axes are concurrent and correspond to the three rotations allowed by the gleno-humeral joint:

- 1) Axis 1 is the shoulder abduction/adduction
- 2) Axis 2 is the internal/external rotation
- 3) Axis 3 is the shoulder flexion/extension.

The fourth axis is the elbow flexion/extension.

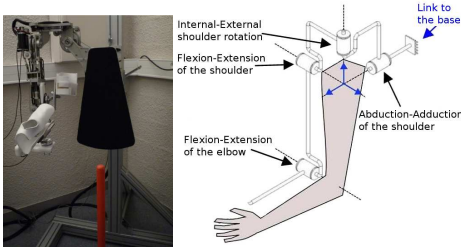


Fig. 3. ABLE exoskeleton and its kinematics.

The exoskeleton is connected to the human arm through two fixations, one being mounted on the arm above the elbow and the second one – on the wrist, as shown on figure 3. At each fixation point, four passive DOFs are added to avoid hyperstaticity [22]. Thanks to two six-axis force/torque (F/T) sensors (one ATI Nano 43 and one ATI Nano 36), interaction forces can be measured at each attachment point.

The control law (20) is implemented on a real time controller, using a PC104 with an endowed 3 channel joint board, under RTLinux operating system. The control loop runs at 1 kHz and data (joint positions/speeds/torques, and torques/forces from sensors) are recorded for post treatment at 100 Hz.

A conventional gravity and friction compensation is implemented using only joint encoder measurements. It shall be clear that this compensation is only partial. In particular, static dry friction, for a null joint velocity, is not compensated, whereas only the dynamic friction can be fed to the low level controller.

#### B. Protocol

The study is realized with one male right-handed healthy subject (age:25). The proposed protocol aims to show the ability of the controller to impose a joint speed constraint to the subject.

The subject is installed in the exoskeleton and is asked to point a target with a rod attached to his arm, in front of him, materialized by a point on a rod, eight times for each mode. Each pointing starts at a fixed reference point beside the subject torso. The reaching target is placed in front of him, about 20 cm under and 30 cm left from the starting point.

The protocol takes place in four steps with a different control modes for each :

- 1) In a first step, only gravity compensation is activated on the robot controller. We measure during this movement, like in the four modes, the exoskeleton joint angle values, speeds and interaction forces at the two contact points. From the joint velocity data, we calculate the linear regressions between the different joint velocities taken two by two, and select one among them. We thus identify the matrix  $C$ . In these experiments,  $C$  is chosen with two null components, which means that the addressed synergy concerns only two joints. Experiments with more general constraint using PCA analysis are also investigated and conducted but not presented in this work.
- 2) During the second step the control law (20) is used with the identified constraint matrix  $C$ . The gain  $k$  is set to 1 Nm.s/rad. The coefficient  $\epsilon$  is set to 0 (only the dissipative torque is applied). The subject is asked to perform the same pointing task.
- 3) During the third step, the same task is again performed by the subject but matrix  $C$  coefficients are slightly changed. The coefficient  $\epsilon$  is still set to 0. The subject is asked to perform the same pointing task.
- 4) The fourth step is identical to the third one, except that  $k = 0.4$  Nm.s/rad and  $\epsilon = 0.8$ . This mode aims to show the possibility of reducing the power dissipated by the control law. The subject is asked to perform the same pointing task.

#### C. Results

During the first protocol step, when the subject is asked to make the movement without any constraint, joint velocities are measured. The natural coordinations between joint speeds are shown on figure 4. They are computed, as all the data presented in this part, only for the reaching movement and not for the back-to-home movement.

As explained in part III-B, we are interested in one linear coordination between two joint speeds. Thus a linear regression is calculated for each coordination and the most linear coupling is chosen for the other steps. In this case the coupling between axes 2 (shoulder internal rotation) and 4 (elbow extension) is chosen. The value computed by regression is then set to the constraint matrix  $C$ . Here  $C = [0 \ 0.75 \ 0 \ 1]$ .

Comparison between results for mode 1 and 2 (figure 4 and 5) indicates that the coupling between axes 2 and 4 is now perfectly linear with very little dispersion, while the rest of the 2 by 2 velocities maps is roughly unchanged.

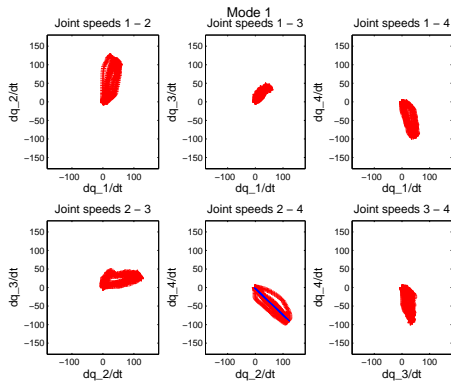


Fig. 4. Joint speed coordinations in free pointing mode.

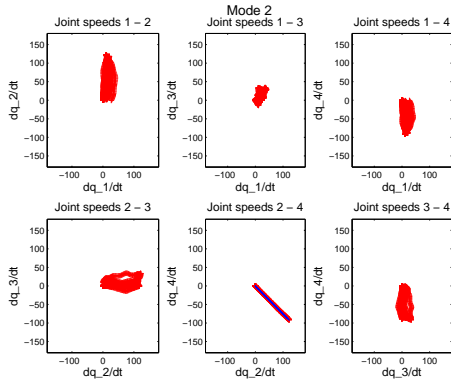


Fig. 5. Joint speed coordinations in natural imposed pointing mode with  $k = 1.0$  and  $\epsilon = 0.0$ .

Speed coordinations 1 – 2 computed for mode 3 and 4 are shown respectively on figure 6 and 7. For these modes, constraint vector has been modified to become  $\mathbf{C}_{\text{modified}} = [0 \ 1 \ 0 \ 3]$ . The coordination gradient is thus three time much as for the natural one.

During step 3, a non natural synergy is imposed by the system. As expected, the subject seems to have more difficulties to respect the non-natural coupling. Observing the interaction force averaged along the motion, as shown on Fig. 8, it appears that the exoskeleton applies to the subject arm more resistive forces to impose the non-natural coupling. Moreover we see that the force levels are similar for non constrained movements (mode 1) and for natural imposed coupling mode (mode 2).

Moreover the mechanical power dissipated by the control law during movement is  $P = \tau_c^T \dot{\mathbf{q}}$ . For each control mode,  $P$  mean is presented on figure 8. For the first mode,  $\tau_c$  is zero and so  $P$  is null. During the second step the torque used to impose the natural coordination is logically small and so  $P$  is small too. For the two non-natural coupling steps it is interesting to notice that, when the  $\epsilon$  scalar modulating the second control torque is 80%, the dissipated energy is clearly reduced.

Although forces applied on the subject arm by the exoskeleton are more important to apply a non-natural coordination, the wrist speed level (corresponding to the robot

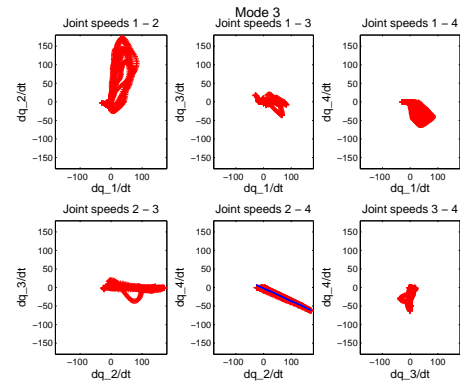


Fig. 6. Joint speed coordinations in non-natural imposed pointing mode with  $k = 1.0$  and  $\epsilon = 0.0$ .

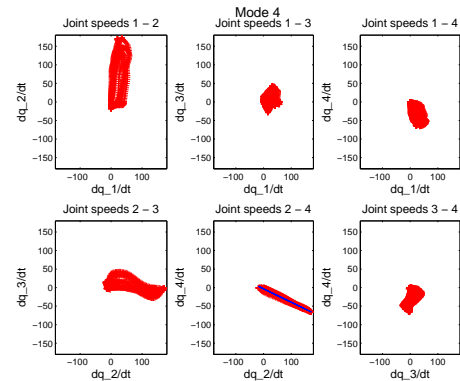


Fig. 7. Joint speed coordinations in non-natural imposed pointing mode with  $k = 0.4$  and  $\epsilon = 0.8$ .

end-effector) is not significantly modified during the different steps as shown on figure 9. It is important to specify that the subject is free to choose the movement duration and the stops duration at each point. He is simply asked to mark a clear stop. It explains the difference of time scale. Similarly, we can observe on figure 10 that wrist (end-point in our case) trajectories is not significantly modified by the coordination constraint during the different modes.

#### IV. CONCLUSION AND PERSPECTIVES

The original control law presented in this paper allows to impose speeds coordination through viscosity constraints without constraining end-point motion. Experimental results

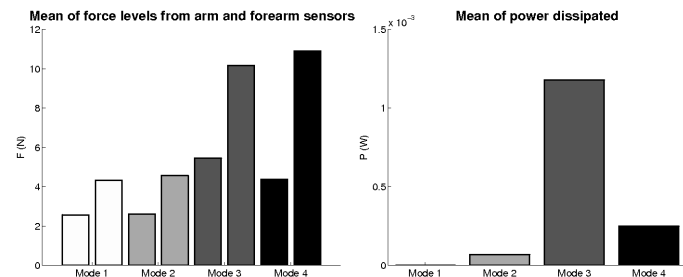


Fig. 8. Mean of force levels and mean of power dissipated for each control mode.

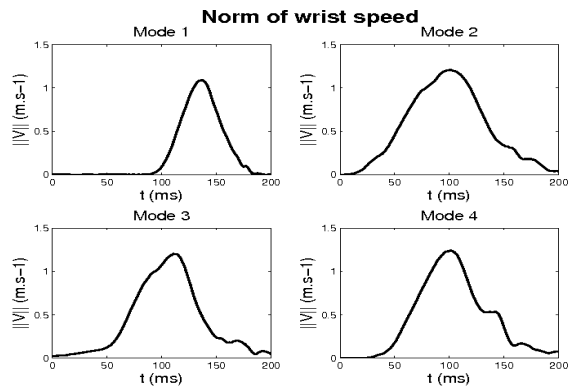


Fig. 9. Norm of the wrist cartesian speed for each control mode.

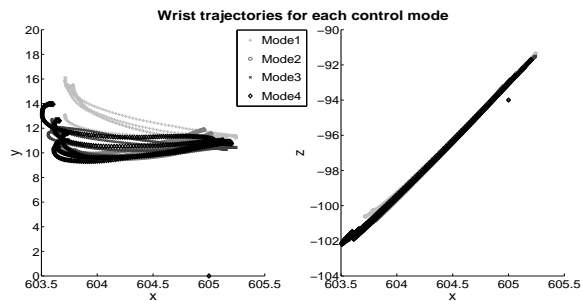


Fig. 10. Wrist trajectory for each control mode. X-Y and X-Z projections.

show that, thanks to redundancy, this control provides to the 4-DOF exoskeleton the ability of imposing a joint coupling relationship to a human arm without disturbing the hand trajectory and velocity. Notably, starting and stopping points of the hand trajectory are not imposed. Moreover the energy dissipated by the control can be reduced down to zero.

We believe that this kind of robotic control can provide an interesting tool for neurorehabilitation. After measuring current pathologic synergies of a patient, a correction, defined in agreement with a therapist, could be applied by the robot. Helping and correcting effects of the system are tunable thanks to the  $\epsilon$  scalar modulating the second torque.

Future investigations will imply a larger number of subjects to evaluate more precisely  $k$  and  $\epsilon$  value effects in the whole workspace. Moreover, we are studying the use of PCA, on arm joint speeds, to express a coordination between all the joints controlled by the exoskeleton. The important next step is to conduct experiments with hemiparetic patients suffering from pathologic synergies. An open problem is to design an appropriate set of correction constraints from observations on a given patient.

## V. ACKNOWLEDGMENTS

The support of the French National Agency for research, ANR, program PSIROB-ROBO-0003, to the Brahma Project is gratefully acknowledged.

## REFERENCES

[1] G. Kwakkel, B.J. Kollen, and H.I. Krebs. Effects of Robot-Assisted therapy on upper limb recovery after stroke: A systematic review. *Neurorehabil Neural Repair*, 22(2):111–121, April 2008.

[2] J. Sivenius, K. Pyorala, OP Heinson, JT Salonen, and P. Riekkinen. The significance of intensity of rehabilitation of stroke—a controlled trial. *Stroke*, 16(6):928, 1985.

[3] R. Riener, M. Frey, M. Bernhardt, T. Nef, and G. Colombo. Human-centered rehabilitation robotics. In *Proceedings of the 9th International Conference on Rehabilitation and Robotics*, pages 319–22, 2005.

[4] M. Schoone, P. van Os, and A. Campagne. Robot-mediated Active Rehabilitation (ACRE) A user trial. In *IEEE 10th International Conference on Rehabilitation Robotics, 2007. ICORR 2007*, pages 477–481, 2007.

[5] S.E. Fasoli, H.I. Krebs, J. Stein, W.R. Frontera, and N. Hogan. Effects of robotic therapy on motor impairment and recovery in chronic stroke. *Archives of physical medicine and rehabilitation*, 84(4):477–482, 2003.

[6] N. Maclean, P. Pound, C. Wolfe, and A. Rudd. Qualitative analysis of stroke patients’ motivation for rehabilitation. *British Medical Journal*, 321(7268):1051, 2000.

[7] MC Cirstea, AB Mitnitski, AG Feldman, and MF Levin. Interjoint coordination dynamics during reaching in stroke. *Experimental Brain Research*, 151(3):289–300, 2003.

[8] L. Dipietro, HI Krebs, SE Fasoli, BT Volpe, J. Stein, C. Bever, and N. Hogan. Changing motor synergies in chronic stroke. *Journal of Neurophysiology*, 98(2):757, 2007.

[9] S. Micera, J. Carpaneto, F. Posteraro, L. Cenciotti, M. Popovic, and P. Dario. Characterization of upper arm synergies during reaching tasks in able-bodied and hemiparetic subjects. *Clinical Biomechanics*, 20(9):939–946, 2005.

[10] N. Bernstein. *The co-ordination and regulation of movements*. Pergamon New York, 1967.

[11] R.A.R.C. Gopura, K. Kiguchi, and Yang Li. SUEFUL-7 : a 7DOF upper-limb exoskeleton robot with muscle-model-oriented EMG-based control. In *Intelligent Robots and Systems, 2009. IROS 2009. IEEE/RSJ International Conference on*, pages 1126–1131, 2009.

[12] EA Brackbill, Y. Mao, SK Agrawal, M. Annapragada, and V.N. Dubey. Dynamics and Control of a 4-dof Wearable Cable-driven Upper Arm Exoskeleton. 2009.

[13] J. He, EJ Koeneman, RS Schultz, DE Herring, J. Wanberg, H. Huang, T. Sugar, R. Herman, and JB Koeneman. RUPERT: a device for robotic upper extremity repetitive therapy. In *Engineering in Medicine and Biology Society, 2005. IEEE-EMBS 2005. 27th Annual International Conference of the*, pages 6844–6847, 2005.

[14] TG Sugar, J. He, EJ Koeneman, JB Koeneman, R. Herman, H. Huang, RS Schultz, DE Herring, J. Wanberg, S. Balasubramanian, et al. Design and control of RUPERT: a device for robotic upper extremity repetitive therapy. *IEEE Transactions on Neural Systems and Rehabilitation Engineering*, 15(3):336–346, 2007.

[15] M. Laffranchi, N.G. Tsagarakis, F. Cannella, and Caldwell D.G. Antagonistic and series elastic actuators : a comparative analysis on the energy consumption. In *Intelligent Robots and Systems, 2009. IROS 2009. IEEE/RSJ International Conference on*, pages 5678–5684, 2009.

[16] T. Nef and R. Riener. ARMin—design of a novel arm rehabilitation robot. In *Rehabilitation Robotics, 2005. ICORR 2005. 9th International Conference on*, pages 57–60, 2005.

[17] M. Mihelj, T. Nef, and R. Riener. A novel paradigm for patient-cooperative control of upper-limb rehabilitation robots. *Advanced Robotics*, 21(8):843–867, 2007.

[18] P. Garrec, JP Friconeau, Y. Measson, and Y. Perrot. ABLE, an innovative transparent exoskeleton for the upper-limb. In *IEEE/RSJ International Conference on Intelligent Robots and Systems, 2008. IROS 2008*, pages 1483–1488, 2008.

[19] N. Hogan. Impedance Control: An Approach to Manipulation: Part I—3. *ASME Journal of Dynamic Systems, Measurement and Control*, 107(1):1–24, 1985.

[20] C.R. Carignan, M.P. Naylor, and S.N. Roderick. Controlling shoulder impedance in a rehabilitation arm exoskeleton. In *IEEE International Conference on Robotics and Automation Pasadena, 2008*.

[21] T. Flash and N. Hogan. The coordination of arm movements: an experimentally confirmed mathematical model. *Journal of neuroscience*, 5(7):1688, 1985.

[22] N. Jarrasse and G. Morel. A formal method for avoiding hyperstability when connecting an exoskeleton to a human member. In *Robotics and Automation, 2010. ICRA 2010. IEEE International Conference on*, 2010.